



HAL
open science

Non Monotonous Product Distribution Dependence on Pt/gamma-Al₂O₃-Cl Catalysts Formulation in n-Heptane Reforming.

Olivier Said-Aizpuru, Ana Batista, Christophe Bouchy, Vittorio Petrazzuoli, Florent Allain, Fabrice Diehl, David Farrusseng, Franck Morfin, Jean-Francois Joly, Aurélie Dandeu

► **To cite this version:**

Olivier Said-Aizpuru, Ana Batista, Christophe Bouchy, Vittorio Petrazzuoli, Florent Allain, et al.. Non Monotonous Product Distribution Dependence on Pt/gamma-Al₂O₃-Cl Catalysts Formulation in n-Heptane Reforming.. ChemCatChem, 2020, 12 (8), pp.2262-2270. 10.1002/cctc.201902260 . hal-02544492

HAL Id: hal-02544492

<https://hal.science/hal-02544492v1>

Submitted on 15 Jun 2020

HAL is a multi-disciplinary open access archive for the deposit and dissemination of scientific research documents, whether they are published or not. The documents may come from teaching and research institutions in France or abroad, or from public or private research centers.

L'archive ouverte pluridisciplinaire **HAL**, est destinée au dépôt et à la diffusion de documents scientifiques de niveau recherche, publiés ou non, émanant des établissements d'enseignement et de recherche français ou étrangers, des laboratoires publics ou privés.

Non monotonous product distribution dependence on Pt/ γ -Al₂O₃-Cl catalysts formulation in *n*-heptane reforming.

Olivier Said-Aizpuru,^[a,b] Ana T.F. Batista,^[a] Christophe Bouchy,^[a] Vittorio Petrazzuoli,^[a] Florent Allain,^[a] Fabrice Diehl,^[a] David Farrusseng,^[b] Franck Morfin,^[b] Jean-François Joly,^[a] and Aurélie Dandeu^{*[a]}

Abstract: The synthesis of 19 carefully selected Pt/ γ -Al₂O₃-Cl formulations was followed by high-throughput catalytic testing in order to unravel the effect of an active phase formulation change on *n*-heptane reforming performances. Pt/ γ -Al₂O₃-Cl catalysts were prepared with different Pt (0.3-1%_{wt}) and Cl (0.1-1.4%_{wt}) contents and using two γ -Al₂O₃ supports so that both sites concentrations and sites locations at the crystallite surface vary among the catalyst pool. Catalytic tests were conducted in mild conditions for a comparison of catalysts in kinetic regime. Results show that Pt and Cl concentrations control the competition between hydroisomerisation, hydrogenolysis and hydrocracking pathways. Aromatisation, on the contrary, is poorly affected by formulation changes. Non-monotonous trends linking Pt/Cl ratio to isomerisation selectivity are found for both γ -Al₂O₃ supports. This study provides new insights for the description of bi-functional transformations in catalytic naphtha reforming.

1. Introduction

Catalytic naphtha reforming overall process global performances are intimately linked to the control of the catalyst selectivity towards branched paraffins and aromatic compounds.^[1] These transformations preferably occur through bi-functional mechanisms enabling proton and hydrogen transfers.^[2,3] The choice of the fresh catalyst formulation as well as its regeneration conditions are paramount process operating issues and depend on the targeted aromatics and isoparaffins selectivity.^[1,4] There is therefore a strong motivation for methods enabling the prediction of active phase formulation impact on catalyst performance. A better understanding of this issue shall also provide valuable information for process optimisation and operation.

Bi-functional redox/acidic catalytic processes are widespread in the refining industry. Hydroisomerisation or hydrocracking catalysts both exhibit a metallic phase (affording hydro/dehydrogenations) associated to acid sites located on the

support (usually zeolites or SiO₂/Al₂O₃). Those catalysts are often designed, compared and optimised on the basis of criteria such as *site balance*^[5-7], *site intimacy*^[8-10], or *support porous structure*^[11,12]. Applying these concepts to the description of reforming catalysts is challenging. First, γ -Al₂O₃ supports present in practice less organised surfaces than zeolites.^[13] Second, naphtha reforming transformations involve a weak acidity and are predominantly afforded on the metallic phase. The physical characterisation of the active phase is challenging and hardens the identification of active sites and their investigation.

Typical catalysts correspond to a reduced metallic phase (Pt sub-nanometric particles combined or not with other metals) supported on a weak acidic support (chlorinated γ -Al₂O₃).^[1,14] Direct observation of the metallic phase requires high resolution electron microscopy techniques.^[15,16] γ -Al₂O₃ surface exhibits hydroxyl groups and uncoordinated Al atoms that are respectively potential Brønsted and Lewis acid sites. Chlorine fixation is generally described as the exchange of a Cl atom with a surface hydroxyl group.^[17,18] This phenomenon leads to an overall increase in acidity that is either explained by electron withdrawing effect^[19] or by the disturbance of the H-bond network at the alumina surface^[20]. Chlorine also interacts with the metallic phase and contributes to the stabilisation of Pt particles.^[18] The impact of chlorine on platinum intrinsic reactivity through potential electronic effect is still debated in various cases including hydrocarbon oxidation^[21,22] or hydro-dehydrogenation^[18,23].

Catalytic testing is often carried on model compounds instead of full naphtha cuts.^[24,25] This strategy helps to better understand surface transformations by simplifying the reaction network or mitigating undesired phenomena such as the formation of a carbonaceous deposit. Catalytic naphtha reforming performances can be extrapolated from tests carried on *n*-heptane (nC₇).^[26,27] This molecule is likely to undergo most of reforming transformations (including aromatisation, isomerisation and cracking) while handling a limited number of compounds compatible with detailed kinetic modelling. By comparison with a naphthene rich hydrocarbon cut, *n*-heptane reforming is also less prone to catalytic deactivation by coke deposition.^[28,29] nC₇ is also widely used as a model molecule for the study of other kinds of bi-functional catalysts.^[30-32]

The purpose of this study is to understand the effect of active site localisation and concentration for Pt/ γ -Al₂O₃-Cl catalysts in *n*-heptane reforming. This work compares the catalytic performances in *n*-heptane reforming obtained on a set of nineteen active phase formulations for Pt/ γ -Al₂O₃-Cl systems. Catalysts differ by both Pt content, Cl content and alumina crystallites morphology. The testing strategy is specifically aimed at comparing the intrinsic activity of different catalytic formulations. Experiments are conducted in a range of mild

[a] O. Said-Aizpuru, Dr. A.T.F. Batista, Dr. C. Bouchy, V. Petrazzuoli, Dr. F. Allain, Dr. F. Diehl, Dr. J.F. Joly, Dr. A.Dandeu
IFP Energies Nouvelles
Rond-Point de l'échangeur de Solaize
BP3, 69360 Solaize (France)
E-mail: aurelie.dandeu@ifpen.fr

[b] O. Said-Aizpuru, Dr. F.Morfin, Dr. D.Farrusseng
CNRS, Université de Lyon 1, IRCELYON
2 Avenue Albert Einstein
69100 Villeurbanne

Supporting information for this article is given via a link at the end of the document.

operating conditions. Pt/Cl site molar ratio is hereby proposed as a descriptor for the metal/acid balance of the catalyst. Results exhibit a non-monotonous dependence of product distribution upon this Pt/Cl ratio. The definite explanation of this trending range as well as the conclusive impact of Pt and Cl localisation on the crystallite surface are not provided. Yet, results bring hints for the application of *site balance* or *site intimacy* concepts in naphtha reforming.

2. Methodology

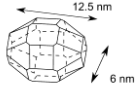
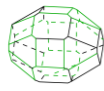
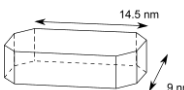
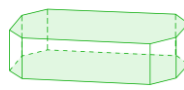
2.1 Presentation of the catalyst library

In bi-functional heterogeneous catalysis, surface site concentration ratios, site locations on the support and inter-site distances are frequently suggested as possible *selectivity descriptors*. Here, the set of samples tested was selected among a collection of catalysts specifically prepared in order to exhibit different Pt/Cl ratios as well as a different spatial repartition of Pt particles and chlorine atoms on the γ -Al₂O₃ crystallite surface. Pt impregnation and chlorine loading adjustment is achieved by the same method (in a fluidized bed) whatever the sample. Hexachloroplatinic acid (H₂PtCl₆.6H₂O) is used as platinum precursor whereas dry oxychlorination or dechlorination with water are used to adjust the chlorine content to the targeted value. Platinum amount varies between 0.3%_{wt} (very close to the industrial value) to 1%_{wt}. Chlorine maximal quantity is equal to 1.4%_{wt} whereas lowest content is around 0.1%_{wt}. Chlorine amounts close to the industrial values (1%_{wt} Cl) are included. Two γ -Al₂O₃ supports are prepared following extrusion and calcination of commercial boehmite gels (Sasol® PuralSB3™ and TH100™). N₂ adsorption and Hg porosimetry indicate fine differences between the supports. PuralSB3™ specific surface and mesoporous diameter are respectively equal to 183±9 nm².g⁻¹ and 9.8±0.02 nm against 149±7 nm².g⁻¹ and 15.1±0.3 nm for TH100™. On the contrary, previous electronic microscopy observations revealed significant crystallite size and morphology differences between the two supports. Crystallites obtained with PuralSB3™ samples are “roundish” or “egg-shaped”.^[33] They are referred to as P-egg crystallites. TH100 based crystallites are bigger and exhibit wider facets as well as shorter overall cumulated edge length.^[33] These crystallites are called T-flat. Geometric representations of the two crystallites with average dimensions are displayed in Table 1.^[33]

X-ray Fluorescence Spectroscopy (XFS) is used to measure the mass amount of Pt and Cl per gram of catalyst. Direct investigation of the metallic particles was afforded by high-resolution electronic microscopy techniques on reduced system. Metallic phase observation^[34] is in overall agreement with thirteen Pt atoms Density Functional Theory (DFT) based particle models predictions that are often suggested when it comes to these systems.^[18,35] Whatever the sample, Pt dispersion values around 0.85 are calculated following H₂/O₂

titration. A fine characterisation of chlorine localisation on the γ -Al₂O₃ surface as well as its interaction with surface hydroxyls was afforded by Batista *et al.* thanks to a multi-technique approach coupling ¹H NMR and DFT calculations. Results indicate that the repartition of chlorine on γ -Al₂O₃ is not uniform. Based on a new ¹H NMR assignment of surface hydroxyls including γ -Al₂O₃ crystallite edges, authors found that chlorine/hydroxyl exchange is energetically favoured in the case of terminal hydroxyls (μ_1 -OH) at the edge (intersection) between (100) and (110) surfaces. According to this new NMR assignment, authors observed that with both chlorinated P-egg and T-flat systems (up to 1.4%_{wt} Cl), chlorine atoms are preferentially located on crystallite edges. In the case of T-flat-1.4%_{wt}Cl catalysts only, the total edge sited are not sufficient to host all Cl atoms and some facet positions must be filled. Taking into account shape differences between T-flat and P-egg crystallites, this preferential location of chlorine on edges may have an impact on the relative localisation between platinum particles and chlorine atoms.^[33]

Table 1. Catalyst library features and nomenclature.

Support	Crystallite proposed morphology ^[33]	Name*	Representation ^[33]
P-egg		P-egg_x% _{wt} Pt_y% _{wt} Cl	 Green: preferential Cl location Ex: P-egg_1.4% _{wt} Cl catalysts
T-flat		T-flat_x% _{wt} Pt_y% _{wt} Cl	 Green: preferential Cl location Ex: T-flat_1.4% _{wt} Cl catalysts

* x varies between 0.3 and 1 %_{wt}, y varies between 0.1 and 1.4%_{wt}

2.2 Catalytic testing strategy

One can distinguish two principal *n*-heptane reforming catalytic testing strategies. Tests may be conducted close to industrial reactor inlet conditions that is to say up to 500°C and over a catalyst that presents a significant amount of coke (more than 5%_{wt}). The aim of these experiments is typically to estimate process catalytic performances^[27], to estimate the impact of various factors on coking phenomena^[28,36,37] and to study catalyst regeneration^[23]. Instead, catalysts can be deliberately tested in a broad range of contact times and partial pressures and at lower temperatures (up to 450°C) to hinder coke deposition. These experimental strategies are typically used in intrinsic kinetic studies.^[26,38–40]

Yield structures obtained in mild conditions are dominated by isomerisation and cracking products. Naphthene proportion is

comprised between 1 and 2%_{mol} and aromatic yields are lower than 25%_{mol}. In severe conditions, yield structures can be significantly different. For instance, Beltramini *et al.* report toluene yields that are up to 80%_{mol} at 515°C, weight hourly space velocity (WHSV) equal to 6 h⁻¹ and after a dedicated accelerated aging procedure.^[41]

Table 2. Ranges of operating condition explored in nC₇ reforming.

Condition	Range	Unit	Comment
Temperature	[390-430]	°C	<450 to limit coking
Total pressure	{5;10}	barg	
H ₂ /nC ₇	{3;5}	mol/mol	>3 to limit coking
Contact time	[3.75-46]	g _{catal} ·min·g ⁻¹ _{nC₇}	Overlaps between contact times obtained at different flow to investigate the effect of reagent velocity
WHSV	[1.3-16]	g _{nC₇} ·h ⁻¹ ·g _{catal} ⁻¹	
nC ₇ inlet flow	[0.3-3.75]	g·h ⁻¹	
Catalyst mass	[75-150]	mg	

Here, contact times, temperatures, total pressure and H₂/nC₇ inlet molar ratio are explored in a range of values representative of mild reforming conditions in order to explore low and middle conversion levels and to alleviate catalyst deactivation so that the intrinsic kinetics of the catalysts are compared (see Table 2). Tests are conducted on a high-throughput catalytic testing set-up (Avantium Flowrence™) equipped with eight parallel fixed bed reactors of 2 mm inner diameter. The geometry of the system permits to test small quantities of catalyst (around 100 mg) and allows for the use of an ideal isothermal plug-flow reactor model, which is adequate to the measurement of intrinsic catalytic reactivity.

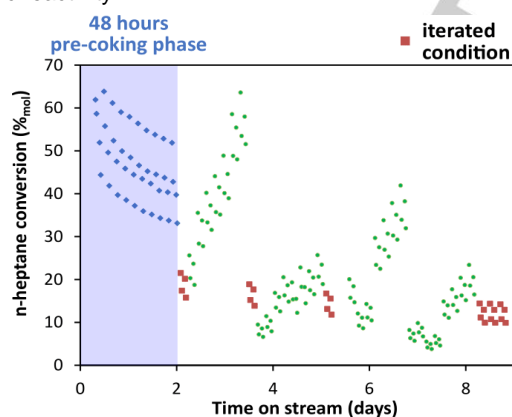


Figure 1. nC₇ conversion on P-egg_0.3%_{wt}Pt_1.3%_{wt}Cl. Blue points correspond to the pre-coking equilibration phase, brown points to the iterated condition (at 390°C, 10 barg, nC₇/H₂ molar ratio equals to 5 and an inlet nC₇ mass flow of 0.2 g·h⁻¹ for each reactor) and green points to the exploration of different operating conditions. Operating conditions ranges are given in Table 2 and detailed protocol is described in ESI.

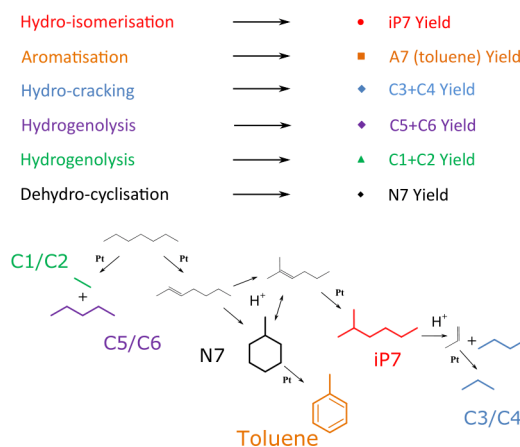
Once loaded in the reactors, catalysts are first reduced for two hours at 500°C under H₂ flow. Then, a preliminary 48 hours pre-coking phase is required in order to increase the stability of catalytic performances. Later in the test, activity loss and selectivity variations due to time on stream is probed by iterating

periodically during the run an identical condition (at 390°C, 10 barg, nC₇/H₂ molar ratio equals to 5 and an inlet nC₇ mass flow of 0.2 g·h⁻¹ for each reactor). Figure 1 presents the variation of conversion obtained for a given catalyst when this standard testing protocol is applied (operating conditions ranges are displayed in Table 2). Product distribution can be measured from on-line gas chromatography analysis at each condition variation all along the standard testing protocol. Further details regarding the testing protocol and the experimental set-up are given in the Electronic Supplementary Information (ESI).

3. Catalytic testing results

3.1 Results obtained for one example catalyst: P-egg_0.3%_{wt}Pt_1.4%_{wt}Cl

As illustrated in Figure 1, broad *n*-heptane conversion levels are successfully explored in different conditions during the test. Once the testing protocol is complete, the dependence of product distribution on the conversion level can be investigated by representing the yield of different products in function of the conversion level (the resulting charts are hereafter called “yield structures”). Analyses distinguish six main families of products that represent between 97.5 and 100%_{mol} of all detected species. As presented in Scheme 1, each family of products can be associated to a reaction pathway as listed below: C₇ isoparaffins (hydroisomerisation products, noted iP₇), Toluene (nC₇ aromatisation product, noted A₇), C₇ naphthenes (dehydrocyclisation products, called N₇), C₅+C₆ (hydrogenolysis products), C₃+C₄ (mainly hydrocracking products) as well as C₁+C₂ (hydrogenolysis products). Remaining products are mostly benzene, linear single double bond olefins, traces of C₈ aromatics as well as unknown compounds. According to Scheme 1, most of mentioned *n*-heptane reforming transformations require bi-functional catalysis. Naphthene dehydrogenation and hydrocarbon hydrogenolysis appear as the only mono-functional pathways and are considered to occur on the metal phase.



Scheme 1. Hypothetic pathways leading to the formation of *n*-heptane main reforming product families.

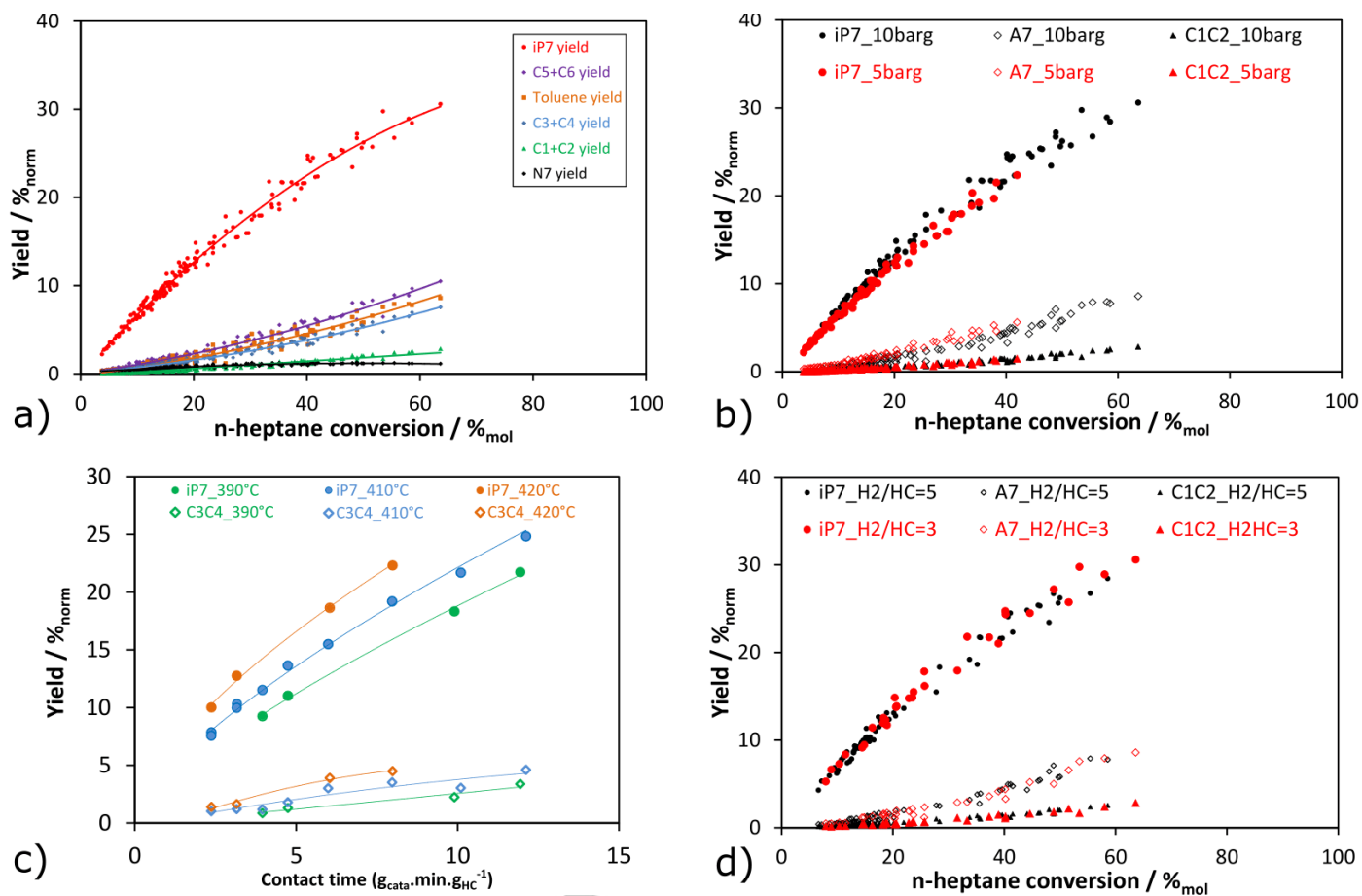


Figure 2 - Catalytic performances obtained for P-egg_0.3%wtPt_1.4%wtCl. a) Yield structure b) Total pressure dependence of iP₇, A₇ and C₁+C₂ products c) iP₇ and C₃+C₄ yields in function of the contact time and at different temperatures. H₂/nC₇ ratio is equal to 5; total pressure is set at 10 barg d) H₂/nC₇ molar ratio pressure dependence of iP₇, A₇ and C₁+C₂ products at 10 barg.

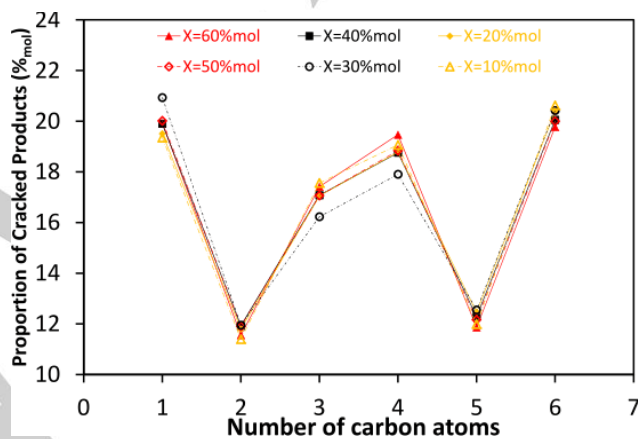


Figure 3. Distribution of cracked products (normalised by the total quantity of cracked products) at different conversion levels and using P-egg_0.3%wtPt_1.4%wtCl catalyst.

This work required to evaluate the competition between the different reforming pathways. Yields were then normalised by carbon atom number using the following expression where F_{CxHy} and Y_{CxHy} , respectively stand for the molar flow and the normalised yield of generic species $CxHy$. $Y_{CxHy} (\%_{norm}) = 100 * xF_{CxHy,outlet} / 7F_{nC7,inlet}$. n -Heptane conversion is noted X_{nC7} and is calculated as $X_{nC7} (\%_{mol}) = 100 / (1 - F_{nC7,outlet} / F_{nC7,inlet})$.

Figure 2 represents the yield structure obtained on P-egg_0.3%wtPt_1.4%wtCl starting from the operation exploration steps (after the 48 hours of stabilisation). One should note that yield structures are plotted irrespectively of operating conditions. On these charts, close overall conversion levels are reached at different P, T, reagent velocities and times on stream. On first approximation, product distributions obtained at a given conversion but for different operating conditions are close. The variety of both operating conditions and times on stream at the same conversion level is nevertheless responsible for the dispersion of yield values around the main trends. Figure 2 b), c) and d) display the dependency of products selectivities upon operating condition variations. Shifting total pressure from 10 to 5 barg has a deep influence on catalyst activity but slightly affects product distribution at a given conversion level (see Figure 2 b)). Similarly, as shown in Figure 2 d), at a given total pressure, the explored H_2/nC_7 inlet ratio variations have a moderate influence on product distribution. According to Figure 2 c), temperature variations between 390°C and 430°C have a more significant impact on the balance between different pathways, which is in agreement with different activation energies for each kind of transformations.

Naphthene yield was found to be systematically lower than 3%_{norm} and is relatively constant. In particular it slightly decreases at conversion values higher than 50%_{mol}. This observation is consistent with the fact that naphthenes are intermediate species in a dehydrocyclisation/aromatisation pathway transforming n -heptane into toluene. As reported by other authors^[38-40], n -heptane reforming product distribution is controlled by the competition between cracking and isomerisation reactions. As soon as a n -heptane molecule is cracked, the lighter (C_6^-) products formed do not undergo aromatisation transformation any longer. Linear paraffin cracking phenomena are usually divided into two families.^[6,7] Hydrocracking results from a multi-step mechanism including isomerisation followed by acid cracking at the vicinity of secondary carbon atom. On the contrary, C-C bond hydrogenolysis is a single step reaction that takes place on metallic sites. The relative activity associated to hydrogenolysis and hydrocracking as well as the nature of the hydrocarbons formed by each pathway is known to depend on the nature of the metal. In the case of n -heptane reforming on Pt/ γ - Al_2O_3 -Cl systems, C_1 , C_2 , C_5 , and C_6 compounds are considered as hydrogenolysis products. Although reduced platinum hydrogenolysis activity is reported to lead to some extent to C_3 and C_4 products, bi-functional hydrocracking is mainly responsible for the formation of these compounds.^[42]

Figure 3 provides the carbon atom distribution of cracking products obtained at different conversion levels on P-egg_0.3%wtPt_1.4%wtCl. Whatever the conversion level, $C_1+C_2+C_5+C_6$ represent more than 60%_{mol} of all cracking products. This repartition underlines the coexistence of both hydrogenolysis and hydrocracking reactions with a predominance of hydrogenolysis.

3.2 Comparison of performances within the catalyst pool

This section presents the variability of catalytic performances over the set of formulations tested. This comparison is aimed at understanding the effect of Pt and Cl content at the crystallite scale on the balance between different reforming pathways. A common legend specified in Figure 4 is used on the graphs presented hereafter. Each active phase formulation is represented by a specific mark shape. Color is chosen to distinguish P-egg catalysts (blue) from T-flat catalysts (red). Hydrogenolysis products resulting from transformations occurring exclusively on the metallic phase, their yield can be taken as an indicator of Pt hydrogenolysis activity. Methane and Ethane yields are representative of both hydrogenolysis of C-C bonds in alpha and beta position of linear paraffins. Therefore, it is expected that surface metal site density is directly correlated to the C_1+C_2 yield. The total number of available/exposed platinum atoms was deduced from the amount of Pt calculated by XFS and the metal dispersion. Figure 5 represents the impact of the total number of available Pt atoms on C_1+C_2 yield extracted in a given condition (H_2/nC_7 equal to 5, 410°C and contact time equal to $10 \pm 1 \text{ g}_{cata} \cdot \text{h} \cdot \text{g}_{nC7}^{-1}$). Results indicate that whatever the chlorine content of the catalyst, the richer the catalytic surface in metallic sites, the higher the C_1+C_2 yield. This effect is higher on T-flat than P-egg crystallites. The amount of Pt also appears as the principal descriptor of overall catalytic activity as illustrated by the comparison between n -heptane conversion levels obtained in an identical condition with distinct catalysts (see Figure 6).

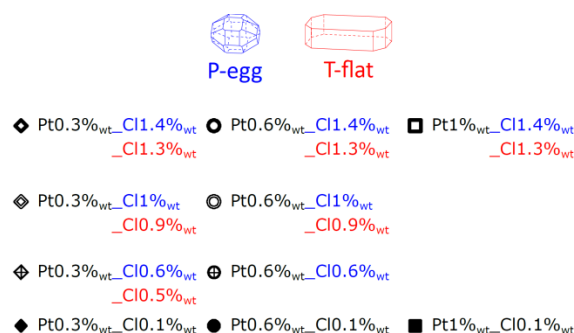


Figure 4. Legend used in order to indicate catalyst formulation.

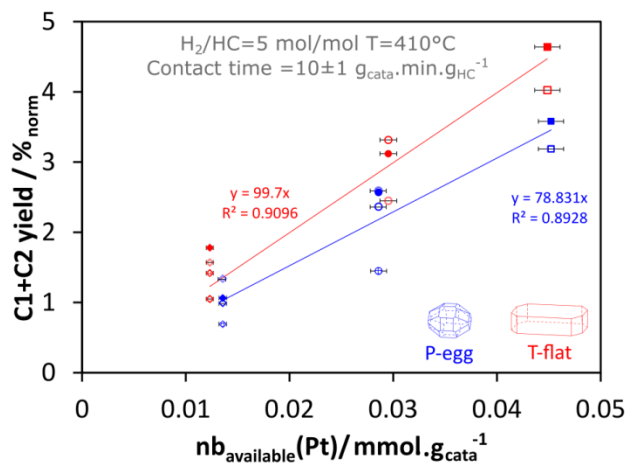


Figure 5. Evolution of C₁+C₂ hydrogenolysis products yields in function of the amount of surface Pt atoms per gram of catalyst at a H₂/nC₇ molar ratio equal to 5, 10 barg total pressure, 410°C and 10 g_{cata}·min·g_{nC7}⁻¹.

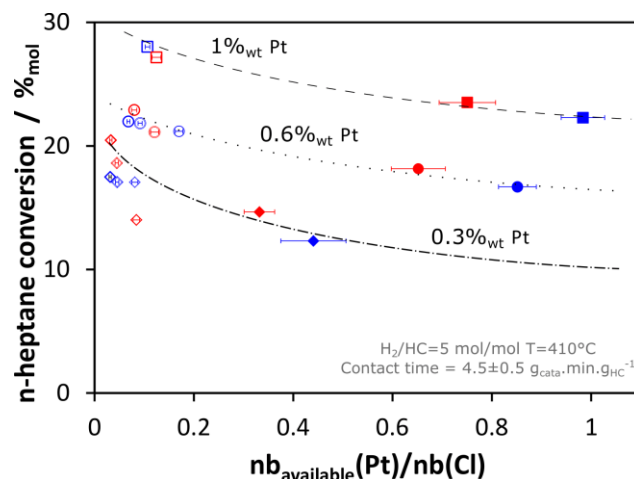


Figure 6. *n*-heptane conversion evolution in function of surface Pt/Cl ratio at H₂/nC₇ molar ratio equal to 5, 10 barg total pressure, 410°C and 10 g_{cata}·min·g_{nC7}⁻¹.

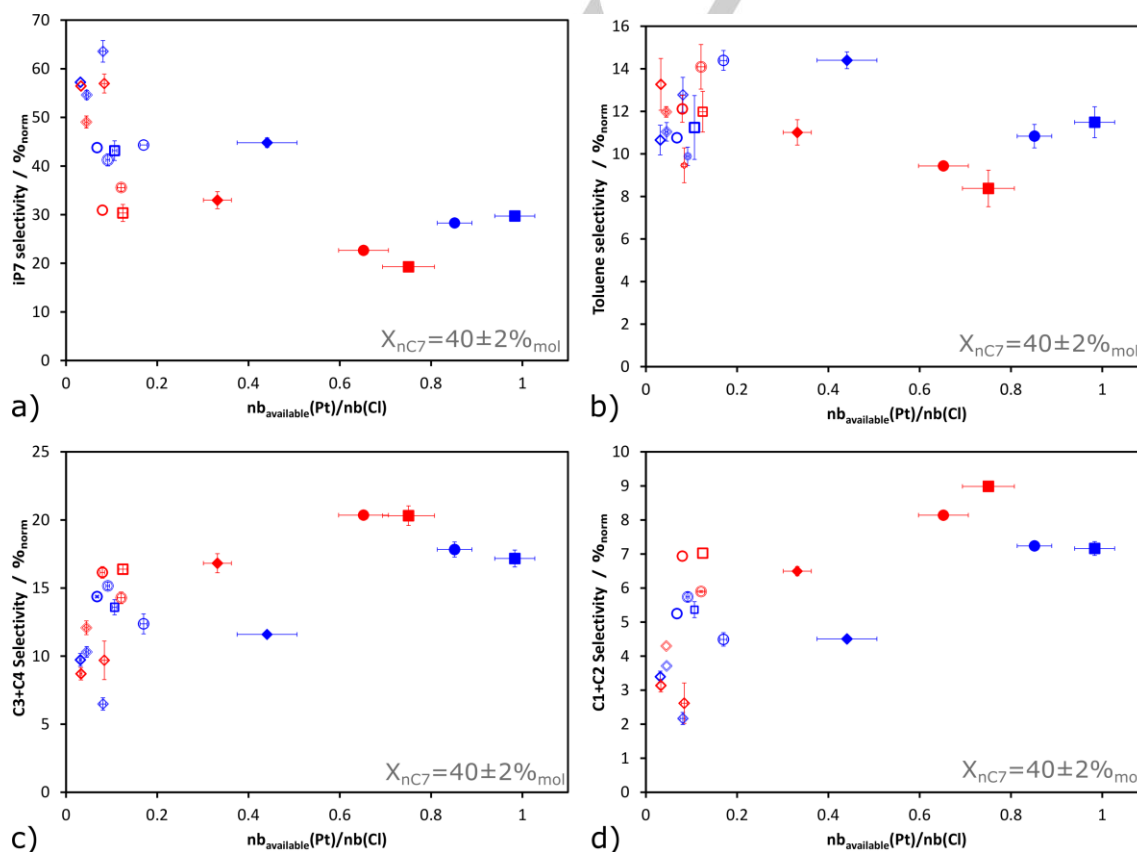


Figure 7. Evolution of the selectivity of different families of products extracted at 40%_{mol} *n*-heptane conversion in function of the surface Pt/Cl ratio. a) iP₇, b) A₇, c) C₃+C₄, d) C₁+C₂.

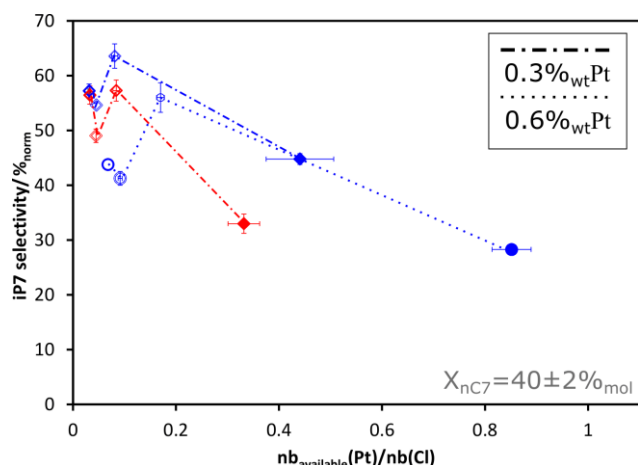


Figure 8. Effect of $nb_{available}Pt/nb(Cl)$ on iP_7 selectivity at different Pt coverages, on P-egg and T-flat supports and at 40% $_{mol}$ nC_7 conversion.

Gamma-alumina supports with a chlorine amount lower than 1.5% $_{wt}$ are weak acidic systems presenting a variety of surface hydroxyls and uncoordinated Al atoms that can act as potential Brønsted or Lewis acid sites. It is very difficult to calculate a Metal/Acid site ratio for classical naphtha reforming catalysts due to a lack of analytical methods for the quantification of acidic sites. Knowing that the addition of chlorine is used to increase the acidity of a reforming catalyst, a global surface Pt/Cl molar ratio is taken in this study as an indicator of Metal/Acid site balance. This Pt/Cl ratio is defined as the total quantity of available Pt atoms per gram of catalyst (Pt atom.g $^{-1}$, as described above) divided by the quantity of Cl atoms per gram of catalysts (Cl atom.g $^{-1}$, inferred from XFS measurements of Cl amount). In the catalyst library, variations of Pt and Cl content lead to the exploration of Pt/Cl ratios from 0.02 to 1.

It was observed that the higher the Pt/Cl ratio (Pt increase + Cl decrease), the higher the selectivity towards cracking products. Figure 7 represents the value of different families of products selectivities at 40% $_{mol}$ n -heptane conversion ($\pm 2\%_{mol}$). The vertical error bars correspond to the selectivity values dispersions in the range of picked-up points. Figure 7 c) and Figure 7 d) show that C_1+C_2 as well as C_3+C_4 selectivities present comparable trends in function of the Pt/Cl ratio. This global increase in both hydrogenolysis and hydrocracking selectivities related to an increase in Pt/Cl ratio is compensated by a loss of n -heptane isomerisation selectivity. However, as highlighted in Figure 8, an optimal isomerisation selectivity is found for intermediate chlorine content samples at a loading of 0.5% $_{wt}$ -Cl.

Similar dependence of n -heptane product distribution on catalysts formulation is observed for both supports. Activity levels in a given operating condition and identical catalyst formulation is roughly the same for both supports. The non-monotonous shape of the trend linking Pt/Cl ratio with C_7 paraffin and cracking selectivities is also the same for both P-egg and T-flat based catalysts. As highlighted in Figure 8, 0.5% $_{wt}$ -Cl catalysts were systematically identified as outliers on the selectivity curves plotted in function of Pt/Cl. That is to say that on both supports and at different amounts of Pt, 0.5% $_{wt}$ chlorine

catalyst were found to be more selective towards C_7 isoparaffins. Aromatisation selectivity at a given conversion shows a bigger dispersion. Average aromatisation selectivity does not present significant differences between catalysts. As presented in Figure 7 b). Pt/Cl also appears a relevant descriptor of catalyst deactivation and selectivity loss among the selected formulations tested in the conditions of this study. Catalyst stability was investigated by comparing the activity and selectivity loss between the first and the last iterated conditions (390°C, 10 barg, nC_7/H_2 molar ratio equals to 5 and 0.2 g.h $^{-1}$ of nC_7 at the reactor inlet). The stability of the catalyst mainly depends on its formulation, with activity loss in the iterating condition ranging from 2% $_{mol}$ (chlorine poor catalysts) to more than 10% $_{mol}$ (for T-flat_0.3% $_{wt}Pt$ _1.3% $_{wt}Cl$). Figure 9 indicates that this activity loss corresponds principally to a loss in isomerisation activity, as cracking and aromatisation activities are more stable throughout the run.

The comparison of product distribution at other n -heptane conversion levels (20% $_{mol}$ and 60% $_{mol}$) as well as the activity measured at other contact times leads to identical observations.

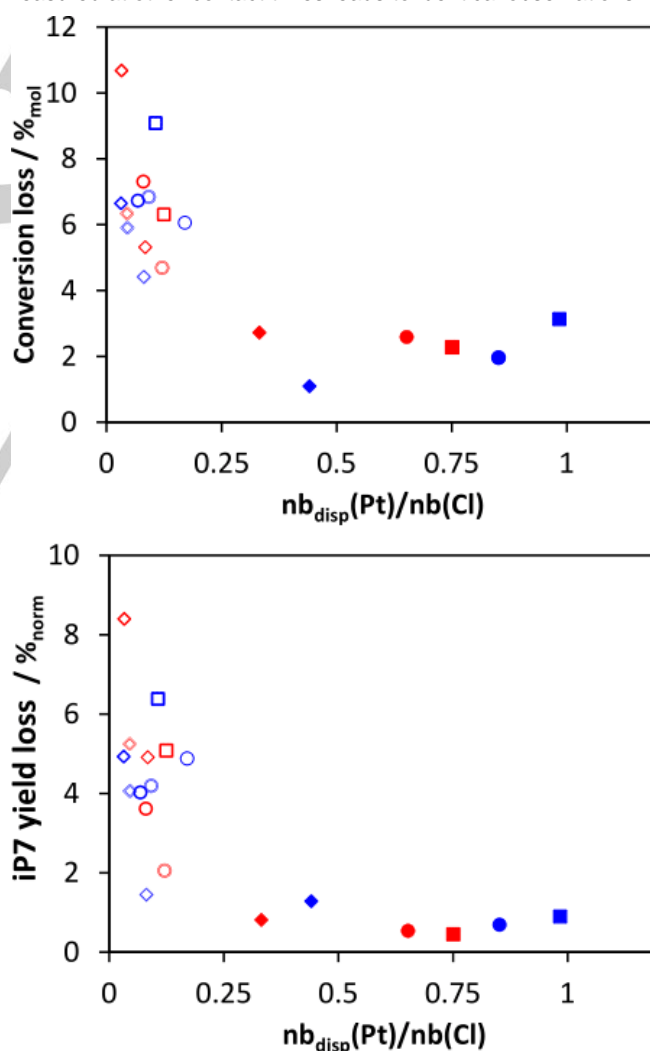


Figure 9. Conversion and iP_7 yield losses between the first and the last iterated condition analysis.

4. Discussion

In this study, *n*-heptane reforming catalytic performances are globally driven by the competition between C₇ paraffin isomerisation, on the one hand, and hydrogenolysis and hydrocracking, on the other hand. The higher the Pt loading on the catalyst, the higher its activity and its selectivity towards hydrogenolysis and hydrocracking products. It is suggested that the reaction system is dominated by transformations on the metallic phase and that an enrichment in Pt leads to the hydrogenolysis of intermediates otherwise involved in bi-functional transformations. It is to be noted that this phenomenon is opposite to what is reported for Pt/zeolites hydroisomerisation catalysts. This second family of bi-functional catalysts behaves differently with a stronger acidity leading to acid cracking reactions. For hydrocracking catalysts, an increase in the number of metal sites increases the selectivity in isoparaffins until a plateau is reached.^[43,44]

Here, aromatisation selectivity is poorly affected by the formulation changes. This first suggests that aromatisation is not limited by metal phase reactions as a three fold increase in metal site density does not significantly affect aromatisation selectivity. One can also advocate that the potential acid sites required for the heptane dehydrocyclisation step are already present on 0.1%_w-Cl catalyst and that they are not necessarily affected by a further increase in chlorine content. The hypothesis of a direct cyclisation step on the metallic phase (though reported as rare and slow) cannot be ruled out.^[3,45]

T-flat and P-egg catalysts were tested in the same conditions and with equal site coverages. The effect of formulation change on product distribution is comparable. On the whole, P-egg catalysts were found to be more selective towards isomerisation than T-flats solids and the difference between the two families of catalysts is bigger at low chlorine coverages (0.1%_w-Cl systems). Site geometric repartition at the crystallite scale (and possibly site intimacy) might be responsible for this selectivity discrepancy. Intrinsic acid site strength could also be taken into consideration. Moreover, it is to be kept in mind that P-egg and T-flat alumina supports present variable textural properties and reactant diffusion differences are not to be excluded. Sensitivity towards coke deposition is an additional potential cause of performance disparity between the catalytic systems owing to their distinct mesoporous diameter value.

For the best of our knowledge, the peculiar reactivity observed for intermediate chlorine contents has not been reported so far and cannot be qualitatively explained. The fact that it occurs at the same Cl level on very different supports excludes experimental errors or bias. We can assume that second order phenomena such as intricate relations between chlorine, coke formation and intrinsic metal phase activity could be involved and lead to hydrogenolysis selectivity loss at this specific chlorine coverage.

5. Conclusions

A high-throughput mild conditions *n*-heptane reforming testing campaign was successfully conducted on a pool of Pt/ γ -Al₂O₃-Cl catalysts comprising nineteen formulations. Two sets of catalysts differing by both the textural properties of their support and the spatial repartition of Pt and chlorine (at the same surface concentration) were tested. Product distributions plotted in function of the Pt/Cl ratio presented similar trends for the two families of catalysts. Whatever the support, an increase in Pt content leads to a rise in hydrogenolysis selectivity. This suggests that the competition between mono-functional hydrogenolysis and bi-functional hydroisomerisation is deeply affected by the formulation changes. However, the yield in aromatics did not present a clear dependence upon formulation change and confirms that aromatisation reaction is not limited by dehydrogenation reactions on the metal phase.

At a given Pt/Cl ratio value, one set of formulations (P-egg based catalysts) is systematically more selective towards isoparaffins. The origin of this selectivity gap between supports is unclear. Among the possible explanations, one can propose either an effect of site intimacy, different intrinsic acidity between the two supports or a different sensitivity towards coke formation. The effect of chlorine content variation on reforming selectivity is an industrial issue insofar as dechlorination happens during operation and continuous catalytic recycling technologies enables to tune the chlorine content of the recycled catalyst. Contrary to what Parera *et al.* reported in different conditions (highly coked catalysts tested at 500°C^[27]), this study shows that in mild conditions and over the 0.1-1.4%_w range, the effect of chlorine content on C₇ isoparaffins selectivity in *n*-heptane reforming is not monotonous and suggests the existence of a local optimum around 0.5%_w-Cl.

This work shows that systematic catalytic studies of reforming catalysts are still of importance to gain a better understanding of their complex bi-functional reactivity. *N*-heptane reforming testing appears as a useful strategy to study metal/acid balance for Pt/ γ -Al₂O₃-Cl systems. Complementary reactions can be studied for a deeper investigation of the catalyst reactivity. Methylcyclohexane or methylcyclopentane dehydrogenation to aromatics could be taken as an indicator of hydro/dehydrogenation activity of the metallic phase. Model acid catalysed reaction such as branched olefin isomerisation can shed light on the nature and the strength of acid sites existing at the reforming catalyst surface.

Acknowledgements

The authors would like to thank E.Rosati, C.Guegan, C.Mancia, C.Popelin and A. Berliet for their contribution to catalyst preparation and testing. Catalytic tests were conducted on the high-throughput heterogeneous catalytic platform located on Axel'One Campus facilities.

Keywords: *n*-heptane reforming • Pt/ γ -Al₂O₃-Cl • bi-functional catalysis • selectivity descriptor

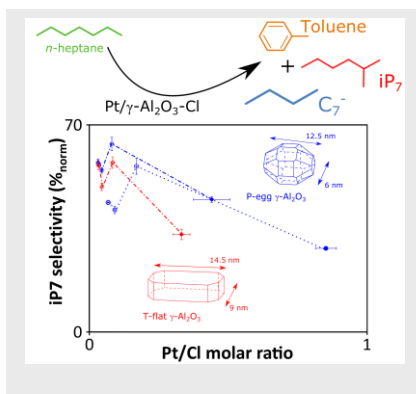
-
- [1] G. J. Antos, A. M. Aitani, *Catalytic naphtha reforming, revised and expanded*, CRC Press, **2004**.
- [2] C. Marcilly, *Acido-basic catalysis: application to refining and petrochemistry*, Technip Ophrys Editions, **2006**, Vol. 2.
- [3] B. H. Davis, *Catalysis Today* **1999**, *53*, 443–516.
- [4] D. Iranshahi, M. Karimi, S. Amiri, M. Jafari, R. Rafiei, M. R. Rahimpour, *Chemical Engineering Research and Design* **2014**, *92*, 1704–1727.
- [5] P. S. F. Mendes, J. M. Silva, M. F. Ribeiro, A. Daudin, C. Bouchy, *Catalysis Today* **2019**, *in press*.
- [6] M. Guisnet, *Catalysis Today* **2013**, *218-219*, 123–134.
- [7] J. Weitkamp, *ChemCatChem* **2012**, *4*, 292–306.
- [8] W. Knaeble, E. Iglesia, *Journal of Catalysis* **2016**, *344*, 817–830.
- [9] P. B. Weisz, *Advances in Catalysis* **1962**, *13*, 137–190.
- [10] J. Zecevic, G. Vanbutsele, K. P. de Jong, J. A. Martens, *Nature* **2015**, *528*, 245–248.
- [11] B. D. Vandegheuchte, J. W. Thybaut, J. A. Martens, G. B. Marin, *Catalysis Science & Technology* **2015**, *5*, 2053–2058.
- [12] J. M. Arroyo, G. G. Martens, G. F. Froment, G. B. Marin, P. A. Jacobs, J. A. Martens, *Applied Catalysis A: General* **2000**, *192*, 9–22.
- [13] M. O. Coppens, G. F. Froment, *Chemical Engineering Science* **1996**, *51*, 2283–2292.
- [14] G. Curtis, V. Haensel, *Reforming process*, **1949**, Google Patents.
- [15] A. I. Frenkel, C. W. Hills, R. G. Nuzzo, *The Journal of Physical Chemistry B* **2001**, *105*, 12689–12703.
- [16] P. D. Nellist, S. J. Pennycook, *Science* **1996**, *274*, 413.
- [17] A. A. Castro, O. A. Scelza, G. T. Baronetti, M. A. Fritzler, J. M. Parera, *Applied Catalysis* **1983**, *6*, 347–353.
- [18] C. Mager-Maury, C. Chizallet, P. Sautet, P. Raybaud, *ACS catalysis* **2012**, *2*, 1346–1357.
- [19] A. Kytökiivi, M. Lindblad, A. Root, *Journal of the Chemical Society, Faraday Transactions* **1995**, *91*, 941–948.
- [20] M. Digne, P. Raybaud, P. Sautet, D. Guillaume, H. Toulhoat, *Journal of the American chemical society* **2008**, *130*, 11030–11039.
- [21] D. Wolf in *Principles and methods for accelerated catalyst design and testing*, Springer, **2002**.
- [22] E. Marceau, H. Lauron-Pernot, M. Che, *Journal of Catalysis* **2001**, *197*, 394–405.
- [23] G. J. Arteaga, J. A. Anderson, C. H. Rochester, *Journal of Catalysis* **1999**, *187*, 219–229.
- [24] C. Kappenstein, M. Guérin, K. Lazar, K. Matusek, Z. Pàal, *J. Chem. Soc., Faraday Trans.* **1998**, *94*, 2463–2473.
- [25] J. H. Sinfelt, J. C. Rohrer, *Journal of Chemical and Engineering Data* **1963**, *8*, 109–111.
- [26] P. A. van Trimpont, G. B. Marin, G. F. Froment, *Applied Catalysis* **1986**, *24*, 53–68.
- [27] G. E. Costa, N. S. Figoli, M. R. Sad, G. Zwiener, L. M. Krasnogor, J. M. Parera, *Reaction Kinetics and Catalysis Letters* **1982**, *20*, 171–174.
- [28] M. Bowker, T. Aslam, M. Roebuck, M. Moser, *Applied Catalysis A: General* **2004**, *257*, 57–65.
- [29] K. Liu, S. C. Fung, T. C. Ho, D. S. Rumschitzki, *Journal of Catalysis* **2002**, *206*, 188–201.
- [30] D. Xu, S. Wang, B. Wu, B. Zhang, Y. Qin, C.-F. Huo, L. Huang, X.-D. Wen, Y. Yang, Y. Li, *ACS applied materials & interfaces* **2019**.
- [31] A. Miyaji, T. Okuhara, *Catalysis Today* **2003**, *81*, 43–49.
- [32] N. Parsafard, M. H. Peyrovi, M. Rashidzadeh, *Microporous and Mesoporous Materials* **2014**, *200*, 190–198.
- [33] A. T. F. Batista, D. Wisser, T. Pigeon, D. Gajan, F. Diehl, M. Rivallan, L. Catita, A. S. Gay, A. Lesage, C. Chizallet, P. Raybaud, *Journal of Catalysis* **2019**, *378*, 140–143.
- [34] W. Sinkler, S. I. Sanchez, S. A. Bradley, J. Wen, B. Mishra, S. D. Kelly, S. R. Bare, *ChemCatChem* **2015**, *7*, 3779–3787.
- [35] C. H. Hu, C. Chizallet, C. Mager - Maury, M. Corral-Valero, P. Sautet, H. Toulhoat, P. Raybaud, *Journal of Catalysis* **2010**, *274*, 99–110.
- [36] V. Y. Tregubenko, K. V. Veretelnikov, A. S. Belyi, *Kinetics and Catalysis* **2019**, *60*, 612–617.
- [37] V. Y. Tregubenko, K. V. Veretelnikov, N. V. Vinichenko, T. I. Gulyaeva, I. V. Muromtsev, A. S. Belyi, *Catalysis Today* **2019**, *329*, 102–107.
- [38] P. A. van Trimpont, G. B. Marin, G. F. Froment, *Ind. Eng. Chem. Res* **1988**, *27*, 51–57.
- [39] P. A. van Trimpont, G. B. Marin, G. F. Froment, *Applied Catalysis* **1985**, *17*, 161–173.
- [40] J. Verstraete, PhD Dissertation, Universiteit Gent, **1997**.
- [41] J. N. Beltramini, E. E. Martinelli, E. J. Churin, N. S. Figoli, J. M. Parera, *Applied Catalysis* **1983**, *7*, 43–55.
- [42] G. C. Bond, *Catalysis by metals*, Academic Press, **1962**.
- [43] T. F. Degnan, C. R. Kennedy, *AIChE Journal* **1993**, *39*, 607–614.
- [44] F. Alvarez, F. R. Ribeiro, G. Perot, y. C. Thomazeau, M. Guisnet, *Journal of Catalysis* **1996**, *162*, 179–189.
- [45] B. H. Davis, P. B. Venuto, *Journal of Catalysis* **1969**, *15*, 363–372.
-

Entry for the Table of Contents (Please choose one layout)

Layout 1:

FULL PAPER

Catalytic tests were carried on in order to unravel the effect of an active phase formulation change on *n*-heptane reforming performances. Results show that with Pt/ γ -Al₂O₃-Cl systems, Pt and Cl concentrations control the competition between hydroisomerisation, hydrogenolysis and hydrocracking pathways. Similar non-monotonous trends linking Pt/Cl ratio to isomerisation selectivity are found for two γ -Al₂O₃ supports. This study provides hints for the description of bi-functional transformations in catalytic naphtha reforming.



Olivier Said-Aizpuru, Ana T.F. Batista, Christophe Bouchy, Vittorio Petrazzuoli, Florent Allain, Fabrice Diehl, David Farrusseng, Franck Morfin, Jean-François Joly, and Aurélie Dandeu*

Page No. – Page No.
Non monotonous product distribution dependence on Pt/ γ -Al₂O₃-Cl catalysts formulation in *n*-heptane reforming.